

THE REFINED PHYSICAL PROPERTIES OF TRANSITING EXOPLANETARY SYSTEM WASP-11/HAT-P-10

XIAO-BIN WANG^{1,2}, SHENG-HONG GU^{1,2,6}, ANDREW COLLIER CAMERON³, YI-BO WANG¹, HO-KEUNG HUT⁴,
CHI-TAI KWOK⁴, BILL YEUNG⁵, AND KAM-CHEUNG LEUNG⁵

¹ Yunnan Observatories, Chinese Academy of Sciences, Kunming 650011, China; shenghonggu@ynao.ac.cn

² Key Laboratory for the Structure and Evolution of Celestial Objects, Chinese Academy of Sciences, Kunming 650011, China

³ School of Physics and Astronomy, University of St Andrews, North Haugh, St Andrews, Fife KY16 9SS, UK

⁴ Hokoon Nature Education Cum Astronomical Centre, Sik Sik Yuen, Hong Kong, China

⁵ Hong Kong Astronomical Society, Hong Kong, China

Received 2013 February 28; accepted 2014 January 30; published 2014 March 18

ABSTRACT

The transiting exoplanetary system WASP-11/HAT-P-10 was observed using the CCD camera at Yunnan Observatories, China from 2008 to 2011, and four new transit light curves were obtained. Combined with published radial velocity measurements, the new transit light curves are analyzed along with available photometric data from the literature using the Markov Chain Monte Carlo technique, and the refined physical parameters of the system are derived, which are compatible with the results of two discovery groups, respectively. The planet mass is $M_p = 0.526 \pm 0.019 M_J$, which is the same as West et al.'s value, and more accurately, the planet radius $R_p = 0.999^{+0.029}_{-0.018} R_J$ is identical to the value of Bakos et al. The new result confirms that the planet orbit is circular. By collecting 19 available mid-transit epochs with higher precision, we make an orbital period analysis for WASP-11b/HAT-P-10b, and derive a new value for its orbital period, $P = 3.72247669$ days. Through an ($O - C$) study based on these mid-transit epochs, no obvious transit timing variation signal can be found for this system during 2008–2012.

Key words: planetary systems – stars: individual (WASP-11/HAT-P-10) – techniques: photometric

Online-only material: color figures

1. INTRODUCTION

Transit events of exoplanetary systems are phenomena in which the planets pass in front of the host stars along the sight line of observers on the Earth, and these events result in brightness variations of the host stars following fixed durations called the planets' orbital periods. Among all detection techniques for discovering the exoplanets, the photometric transit method is one of the most important, and can provide us a unique opportunity to gain insight into the complete properties of exoplanetary systems. Up to now, there were more than 330 planetary systems discovered by the transit method.⁷ Photometric observations for transit events of exoplanets can tell us the sizes and masses of the planets, and then their average densities, which are very important for understanding the formation and evolution of exoplanets (Charbonneau et al. 2000). Furthermore, besides discovering new exoplanetary systems through photometric surveys, photometric follow-up observations for known ones are also very important. The monitoring for discovered transiting exoplanetary systems can let us know whether there are other planets in the same systems, through analyzing the transit timing variation (TTV) and transit duration variation (TDV; Agol et al. 2005; Holman & Murray 2005; Kipping 2009a, 2009b). Moreover, such follow-up observations can permit us to improve the physical parameters of transiting systems (Winn et al. 2009), which are helpful in investigating the details related to exoplanet composition, structure, and evolution. Therefore, we have carried out a monitoring project for known transiting exoplanetary systems at Yunnan Observatories since 2007, and the goals are to identify the TTV or TDV phenomena and refine the physical parameters of selected exoplanetary systems. The first results of our project concern the transiting system HAT-P-24

(Wang et al. 2013); here, we present the results for the system WASP-11/HAT-P-10.

WASP-11b/HAT-P-10b was discovered by two individual groups (Bakos et al. 2009; West et al. 2009) simultaneously, and it is a sub-Jupiter-mass exoplanet. Bakos et al. (2009) derived that its mass and radius are $0.487 \pm 0.018 M_J$ and $1.005^{+0.032}_{-0.027} R_J$, respectively, whereas West et al. (2009) gave a mass of $0.53 \pm 0.07 M_J$ and a radius of $0.91^{+0.06}_{-0.03} R_J$ for this exoplanet. Both of them assumed that the planet orbit is circular ($e = 0$), but their results do not agree with each other very well. The host star GSC 02340–01714 is an early K dwarf and has a brightness $V = 11.89$. We monitored this system at Yunnan Observatories, China from 2008 to 2011, and four transit light curves were obtained. Here, we present the relative analysis results of the WASP-11/HAT-P-10 system by combining our new photometric observations with the photometric and radial velocity (RV) observations in the literature (Bakos et al. 2009; West et al. 2009). In Section 2, we describe the photometric observations and relative data reduction strategy. In Section 3, we introduce the physical parameter analysis using the Markov Chain Monte Carlo (MCMC) technique and the orbital period study using linear fitting to the mid-transit epochs. In Section 4, the new results are discussed. Finally, we give the summary of the new study in Section 5.

2. OBSERVATIONS AND DATA REDUCTION

2.1. Photometric Observations

WASP-11/HAT-P-10 was observed using an Andor CCD camera with a $2\text{ K} \times 2\text{ K}$ chip attached to the 1 m telescope of Yunnan Observatories, China, on 2008 November 22, 2009 November 7, 2010 November 29, and 2011 October 30. During all observing runs, the R filter was used and the field of view was $7/3$. The exposure time varied from 90 s to 300 s due to

⁶ To whom the future correspondence and offprint request will be sent.

⁷ <http://exoplanet.eu>

Table 1
The Observing Log of the Transiting Exoplanetary System
WASP-11/HAT-P-10

Date	Filter	Exposure Time (s)	Number of Points	Precision (mag)
2008.11.22	R	150–250	114	0.00332
2009.11.07	R	100–180	131	0.00218
2010.11.29	R	90	116	0.00313
2011.10.30	R	240–300	48	0.00245

different seeing conditions and instrument statuses; the mirrors of the 1 m telescope had not been coated for a couple of years, so its efficiency decreased gradually. Because there is not an auto-guiding system on this telescope, we had to move the telescope manually from time to time during every observing night so that the position of stars did not change too much in the CCD frame.

In the 2008 observing run, the weather was clear with very good seeing conditions. However, the photometric precision (see Table 1) is not high and there are some fluctuations in the light curve; the above-mentioned manual guiding and very good seeing conditions are probably responsible for this issue. For weather with very good seeing conditions, due to the shortcomings of manual guiding, a sharper stellar image with a smaller pixel area walks across a relatively larger region in the CCD frame during the observation, which changes the local flat field of a star; this results in a larger measurement error for the brightness of the star. In the 2009 observing run, the weather was clear but the seeing conditions were not good, and the photometric precision is high, which implies that the flat-fielding procedure does not affect the results in relatively bad seeing conditions. In the 2010 observing run, the weather was clear and the seeing conditions were not bad, but the telescope control system failed some time in the course of observation, which resulted in an incomplete transit light curve that lacked the whole ingress phase. In the observing run of 2011, the seeing conditions were bad and the weather changed to partly cloudy during the egress phase, so the light curve is also incomplete, losing part of the egress phase. Detailed information on these observations is summarized in Table 1, where the precision is the rms error calculated from the residuals between the observing data and best-fitting model (see Section 3).

2.2. Data Reduction

All of the observed CCD images are reduced according to the standard way by means of the IRAF package,⁸ including image trimming, bias subtraction, flat-field correction, and cosmic ray removal. During this procedure, a master bias image and a master flat-field image are used, which are generated using multiple trimmed frames of bias and flat field, respectively. The instrumental magnitude values of the target star and comparison stars in reduced images are measured by using the APPHOT sub-package of IRAF. In the measurements, we try a series of apertures to measure the magnitude values of all stars, and an optimal aperture is selected for each night so as to get the minimum dispersion for the observed light curve. For the observation made on 2008 November 22, eight comparison stars are selected to model the systematic errors in the photometric data, whereas on 2009 November 7, 2010 November 29, and

2011 October 30, nine comparison stars are selected due to a different field of view in the observations.

2.3. Systematic Error Correction

Because the transit signal of an exoplanet is normally weak, we use coarse decorrelation and SYSREM methods to correct the systematic errors in the photometric data so as to enhance the signal-to-noise ratio of transit events (Collier Cameron et al. 2006; Tamuz et al. 2005). First, the photometric data of all comparison stars in the CCD images are analyzed iteratively using the coarse decorrelation method, during which the possible variable objects and the objects with low precision are identified and excluded. Second, the remaining stable comparison stars with higher precision are used to model the systematic errors in the photometric data with the SYSREM method. In the calculation, 4, 6, 5, and 6 comparison stars are used in the 2008, 2009, 2010, and 2011 observing runs, respectively. We model two systematic effects existing in the photometric data; one is associated with atmospheric extinction, the other is associated with the observation times of CCD images, which are relative to the lunar phase. Then, the target star WASP-11/HAT-P-10's photometric data are corrected using these modeled systematic errors. Because we model the systematic errors using only the selected comparison stars, which does not count the systematic trends of the target star WASP-11/HAT-P-10, there are still systematic trends left in the corrected photometric data of the target star. Thus, we use a straight line or parabolic curve to fit the two outer sides of the transit event for each data set so that we can correct these systematic trends in the data. As for the time stamps of our new photometric data, we convert them from local time to the Barycentric Julian Date under the Coordinated Universal Time (BJD_{UTC}), which is widely used in the study of exoplanetary systems. Using the above steps, we derive the final light curves of the transit events for the system WASP-11/HAT-P-10, which are displayed in Figure 1 and will be used to obtain physical parameters of the planetary system in the next section.

3. ANALYSIS

In order to derive the system parameters of WASP-11/HAT-P-10, we use the MCMC technique (details can be found in Collier Cameron et al. 2007; Pollacco et al. 2008; Enoch et al. 2010) to simultaneously estimate the photometric model of the exoplanet transit event and RV model of the host star's orbital motion with four new transit light curves, Bakos et al.'s (2009) two light curves with high precision and their RV curve, and the RV curve of West et al. (2009). With the Metropolis–Hastings algorithm, the posterior probability distributions of the system parameters are obtained, from which the best values and uncertainties of the physical parameters are derived.

Since the work of Pollacco et al. (2008), the code we used has been updated to cope with both circular and eccentric orbit cases; the adjusted parameters are $\{T_0, P, \Delta F, t_T, b, K_1, e \cos \omega, e \sin \omega\}$. T_0 is the mid-transit epoch, P is the orbital period, $\Delta F = (R_p/R_*)^2$ is the fractional flux deficit during transit when not considering stellar limb-darkening, t_T is the transit duration from the first contact to the fourth one, $b = a(1 - e \cos E_T) \cos i / R_*$ is the impact parameter, K_1 is the semi-amplitude of the RV curve of the host star, e is the orbital eccentricity, and ω is the argument of periastron. Here, we used $e \cos \omega$, $e \sin \omega$ instead of e and ω as the jump parameters to increase the convergence rate for the planetary system with small eccentricity, which is explained clearly in the work of Ford (2005). During our

⁸ IRAF is distributed by the National Optical Astronomy Observatory, which is operated by the Association of Universities for Research in Astronomy, Inc., under cooperative agreement with the National Science Foundation.

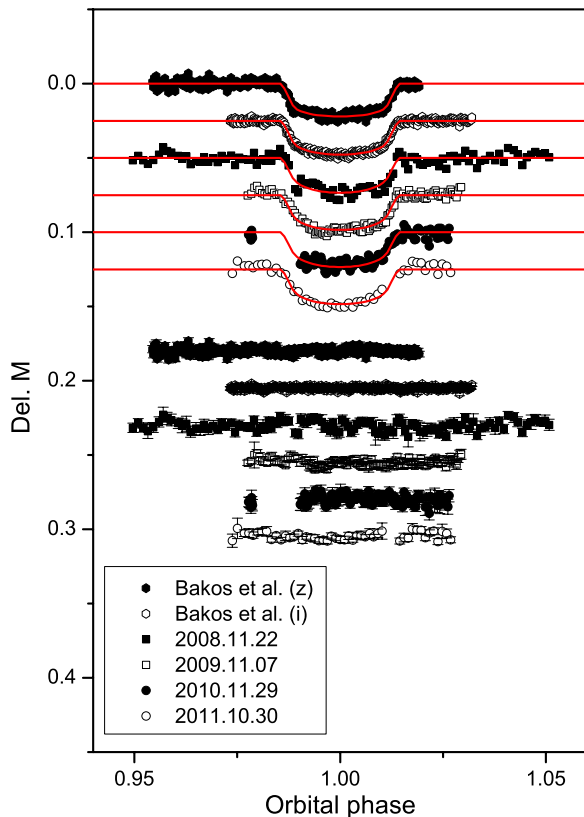


Figure 1. Unbinned light curves of transit events of WASP-11b/HAT-P-10b and the best-fitting model. The upper part represents the observational data points, and the lower one represents the residuals between the observations and model. The solid lines represent the theoretical light curves. For better display, five light curves and all of the residuals between observations and the theoretical curve are offset by different constants.

(A color version of this figure is available in the online journal.)

MCMC analysis, the mass of host star M_* is calculated with the new calibration of Enoch et al. (2010), which is based on stellar effective temperature T_{eff} , metallicity [Fe/H], and stellar density ρ_* , and verified to be reliable and consistent with the results of isochrone analysis.

The transit light curve is modeled using small planet approximation (Mandel & Agol 2002), and the four-coefficient limb-darkening law is used (Claret 2000, 2004). The four limb-darkening coefficients are calculated from Claret’s (2000, 2004) tables of R, i, and z bands through interpolation according to the effective temperature T_{eff} , surface gravity $\log g$, and metallicity [Fe/H] of the host star. The effective temperature $T_{\text{eff}} = 4980$ K and metallicity [Fe/H] = 0.13 of the host star are adopted from Bakos et al.’s (2009) work, which were determined well there. According to our new result of $\log g = 4.58$ derived below and the value $\log g = 4.56$ from Bakos et al. (2009), the surface gravity $\log g = 4.5$ is adopted, which corresponds to an entry of Claret’s (2000, 2004) tables.

First, we analyze the above available transit light curves and RV curves (Bakos et al. 2009; West et al. 2009) simultaneously to get a global solution for photometric and RV observations. The input values of some system parameters for the MCMC analysis are adopted from the results from two discovery papers. The zero-point offsets among the High Resolution Echelle Spectrometer (HIRES), FIES, and SOPHIE RV measurements are calculated and removed during the analysis. From the converged solution, we found that the quantities $e \cos \omega =$

$0.0126^{+0.0308}_{-0.0300}$ and $e \sin \omega = 0.0475^{+0.0585}_{-0.0594}$ are roughly equal to zero within 1σ , which means that the orbit of WASP-11b/HAT-P-10b should be circular. Therefore, we fix the orbital eccentricity at $e = 0$, and re-calculate the above photometric and RV measurements to derive the new global solution. In this solution, a new orbital period is derived. Then, by fixing the orbital period value as the new derived one, the individual transit light curve is analyzed to get the mid-transit epoch for each transit event, which is shown in Table 2.

3.1. Orbital Period Study

In order to obtain a more accurate orbital period value, we collect all available mid-transit epochs with higher precision for the WASP-11/HAT-P-10 system in the literature and the Web site of the Exoplanet Transit Database (ETD),⁹ which were determined using complete and symmetrical transit light curves with higher quality, and are also listed in Table 2. Combining these mid-transit epochs with our five new ones (the mid-transit epoch on 2010 November 29 is not used due to incomplete transit light curve), we analyze the orbital period of the transiting system WASP-11/HAT-P-10 using a linear fitting. The new derived linear ephemeris formula is as follows; here, E represents the orbital cycle number. The relative ($O - C$) diagram is displayed in Figure 2, and the epoch zero point of the ephemeris formula of Bakos et al. (2009) is used as the zero point for the new linear ephemeris formula:

$$\text{BJD}_{\text{UTC}} = 2454759.68706(43) + 3.72247669(181) \times E.$$

3.2. Final Solution

In above subsection, we derived a new accurate orbital period for the system WASP-11/HAT-P-10. Here, we set the orbital period as the new value, $P = 3.72247669$ days, and then perform the MCMC calculation to derive the final values for physical parameters of the system WASP-11/HAT-P-10, based on the above available six transit light curves and the RV data of Bakos et al. (2009) and West et al. (2009). Here, we would like to mention that an RV jitter of 6.5 m s^{-1} is used for RV measurements in the MCMC analysis so as to achieve reduced $\chi^2 = 1$ for the RV data. Because we use three data sets of RV measurements, the RV data set of HIRES is used as a fiducial set in the calculation, and FIES and SOPHIE RV data sets are fitted zero-point offsets relative to the HIRES one. Based on the obtained posterior probability distributions, the best values for the system parameters are derived from their median values, and the uncertainties of the system parameters are taken as 1σ limits of the parameter distributions. The adopted values and the uncertainties of the system parameters are listed in Table 3, and the relative model fitting is illustrated in Figures 1 and 3. One point needs to be mentioned: the center-of-mass velocity γ listed in Table 3 is not the real center-of-mass velocity of the system, it just represents an arbitrary offset value in HIRES RV measurements (for details, see Bakos et al. 2009).

4. DISCUSSION

Based on the new photometric data and published photometric and RV data, we have refined the physical parameters of the transiting exoplanetary system WASP-11/HAT-P-10 using the MCMC technique. Comparing our results with those of Bakos et al. (2009) and West et al. (2009), we can see that the new physical parameters of WASP-11/HAT-P-10 system are

⁹ <http://var2.astro.cz/ETD/>

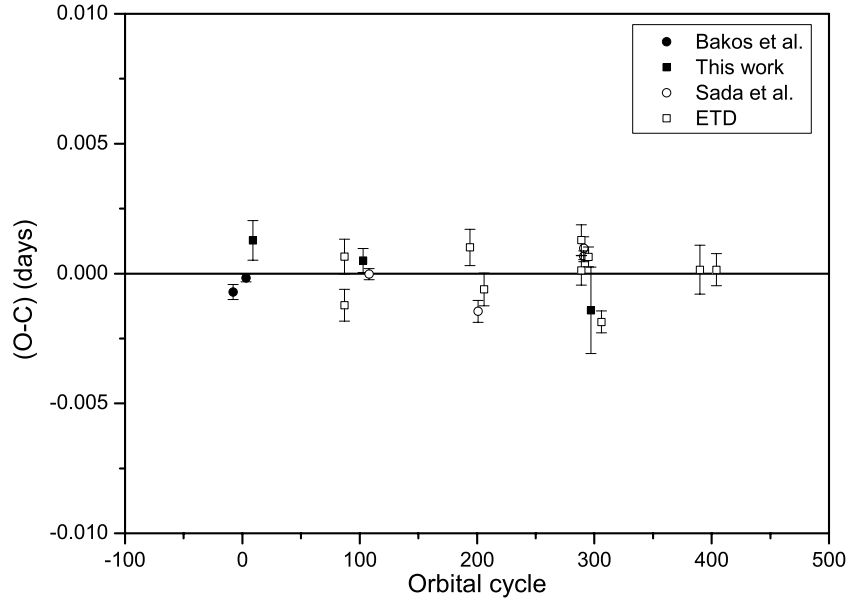


Figure 2. $(O - C)$ diagram for the orbital period study of the WASP-11/HAT-P-10 system. The different symbols represent the sources of transit event observations.

Table 2
The Available Mid-transit Epochs for WASP-11/HAT-P-10

T_0 (days)	σ	Cycle	$(O - C)$ (days)	Source
$BJD_{UTC}2450000+$				
4729.90654	0.00029	-8	-0.00071	This paper (Bakos et al.'s data)
4770.85432	0.00015	3	-0.00017	This paper (Bakos et al.'s data)
4793.19063	0.00076	9	0.00128	This paper
5083.54132	0.00061	87	-0.00122	ETD
5083.54319	0.00067	87	0.00065	ETD
5143.10266	0.00046	103	0.00050	This paper
5161.71452	0.00021	108	-0.00002	Sada et al. (2012)
5481.84855	0.00070	194	0.00101	ETD
5507.90342	0.00042	201	-0.00145	Sada et al. (2012)
5526.51665	0.00063	206	-0.00061	ETD
5835.48294	0.00057	289	0.00012	ETD
5835.48411	0.00059	289	0.00129	ETD
5842.92844	0.00021	291	0.00066	Sada et al. (2012)
5842.92875	0.00044	291	0.00097	Sada et al. (2012)
5857.81832	0.00038	295	0.00064	ETD
5865.26122	0.00166	297	-0.00142	This paper
5898.76306	0.00042	306	-0.00186	ETD
6211.45312	0.00094	390	0.00015	ETD
6263.56779	0.00062	404	0.00015	ETD

consistent with those in the two discovery papers. Our new parameters of the host star are $M_\star = 0.862 \pm 0.014 M_\odot$ and $R_\star = 0.784^{+0.018}_{-0.011} R_\odot$. This mass value is very close to the value of $0.83 \pm 0.03 M_\odot$ of Bakos et al. (2009). This indicates that the mass of the host star derived by the calibration of Enoch et al. (2010) is consistent with the one based on the analysis of the stellar evolution model (Bakos et al. 2009), which means that the new mass calibration of Enoch et al. (2010) is quite robust. The new radius value of the host star is almost the same as the value of $0.79 \pm 0.02 R_\odot$ of Bakos et al. (2009). For the planet WASP-11b/HAT-P-10b, the RV orbital solution suggests its eccentricity $e = 0$ when we combine three data sets of RV measurements from different instruments, which agrees with the results of the two discovery groups based on their own RV data. The new parameters of the planet are $M_p = 0.526 \pm 0.019 M_J$ and $R_p = 0.999^{+0.029}_{-0.018} R_J$. The new planet mass value is the

same as the value of $0.53 \pm 0.07 M_J$ of West et al. (2009), and somewhat larger than Bakos et al.'s (2009) value of $0.487 \pm 0.018 M_J$. The new planet radius value is quite close to that of $1.005^{+0.032}_{-0.027} R_J$ of Bakos et al. (2009) and a little larger than that of $0.91^{+0.06}_{-0.03} R_J$ of West et al. (2009). Consequently, the average density of the planet is $\rho_p = 0.526^{+0.035}_{-0.046} \rho_J$, which is between the values $0.448 \pm 0.039 \rho_J$ of Bakos et al. (2009) and $0.69^{+0.07}_{-0.11} \rho_J$ of West et al. (2009).

The new orbital period value is consistent with that given by Bakos et al. (2009), and a little longer than that of West et al. (2009); it should be more accurate than the old ones because 19 mid-transit epochs derived from the complete transit light curves with higher precision are involved in the analysis. Figure 2 shows the residuals of the observed mid-transit epochs compared to their linear model. From the distribution of $(O - C)$

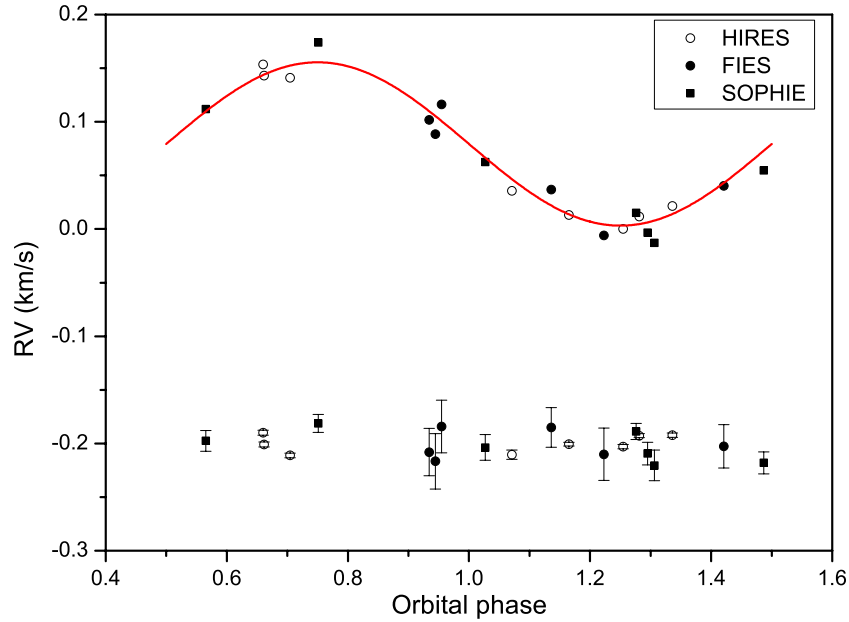


Figure 3. Radial velocity curve and relative model fitting. Phase 1 corresponds to mid-transit. The symbols are used to identify the different RV measurements, and the fitted zero-point offsets relative to HIRES RV measurements are removed for FIES and SOPHIE ones. For the sake of clear display, the residuals between observations and the theoretical curve are offset by a constant and plotted in the bottom.

(A color version of this figure is available in the online journal.)

Table 3
The Physical Parameters and 1σ Error Limits for the Transiting System WASP-11/HAT-P-10

Parameter	Symbol	Value	Unit
Transit epoch	T_0	$BJD_{UTC}2454808.07904^{+0.00012}_{-0.00011}$	days
Orbital period	P	$3.72247669 \pm 0.00000181$	days
Planet/star area ratio	$(R_p/R_*)^2$	$0.01717^{+0.00022}_{-0.00016}$	
Transit duration	t_T	$0.1078^{+0.0006}_{-0.0004}$	days
Impact parameter	b	$0.185^{+0.094}_{-0.107}$	R_*
Stellar reflex velocity	K_1	$76.16^{+2.67}_{-2.58}$	m s^{-1}
Center-of-mass velocity	γ^a	$79.33^{+0.51}_{-0.49}$	m s^{-1}
Orbital inclination	i	$89.138^{+0.503}_{-0.470}$	degrees
Orbital semi-major axis	a	0.04473 ± 0.00024	AU
Stellar mass	M_*	0.862 ± 0.014	M_\odot^b
Stellar radius	R_*	$0.784^{+0.018}_{-0.011}$	R_\odot^b
Stellar density	ρ_*	$1.789^{+0.072}_{-0.116}$	ρ_\odot
Planet radius	R_p	$0.999^{+0.029}_{-0.018}$	R_J^b
Planet mass	M_p	0.526 ± 0.019	M_J^b
Planet density	ρ_p	$0.526^{+0.035}_{-0.046}$	ρ_J
Planet temperature	T_{eq}	$1006.5^{+16.4}_{-14.6}$	K

Notes.

^a The center-of-mass velocity γ is not the real center-of-mass velocity of the system, it just represents an arbitrary offset value in HIRES RV measurements (for details, see Bakos et al. 2009).

^b $M_\odot = 1047.67 M_J$, $R_\odot = 9.96 R_J$.

values, the linear model fits the observed mid-transit epochs well, the rms of the $(O - C)$ values is 0.000967 days (83.55 s), and no significant TTV signal can be identified. Thus, no obvious TTV phenomenon can be inferred from the present $(O - C)$ analysis of orbital period for WASP-11b/HAT-P-10b.

On the other hand, even if there is no obvious periodic signal in the $(O - C)$ diagram, we still can estimate the probability of a companion existing in the WASP-11/HAT-P-10 system if

only considering the light travel time (LTT) effect (Irwin 1952). Assuming a companion is moving with an orbital period of 5 yr in the outer circular orbit, if we take a semi-amplitude of 0.000484 days (half of above rms of the $(O - C)$ values, close to the typical precision of a mid-transit epoch we used) for the LTT effect, the mass function of the companion will be $f(m) = 0.0247 M_J$ using the following well-known formula; here, M_1 , M_2 , and M_3 represent the mass of the host star, transiting planet, and outer companion, respectively; i_3 represents the inclination of orbital plane of the companion; a_{12} is the semi-major axis of the transiting pair; P_3 is the orbital period of the companion; and G is the gravitational constant. If the companion is in a co-planar orbit with the transiting system, we can derive its mass as $27.76 M_J$, which is very large compared with WASP-11b/HAT-P-10b, and will make the mass center of the WASP-11/HAT-P-10 system exhibit obvious RV variation. However, there is no such evidence when analyzing the RV data of WASP-11/HAT-P-10. Through the above analysis, we know that the semi-amplitude of the LTT effect should be much smaller than above assumed value if the companion is a Jupiter-like planet. Therefore, it is almost impossible to detect an extra planet with about Jupiter mass in the outer orbit of a normal transiting exoplanetary system using the LTT effect, which should be very small and hard to identify due to the detection limit:

$$f(m) = (M_3 \sin i_3)^3 / (M_1 + M_2 + M_3)^2 = 4\pi^2 (a_{12} \sin i_3)^3 / G P_3^2.$$

To investigate TDV for the WASP-11/HAT-P-10 system, we need a series of complete transit light curves recorded in the same photometric band so that their transit durations can be compared with each other. Actually, we obtained four transit light curves through the R filter from 2008 to 2011, and two of them (2010 and 2011) are not complete due to an instrument failure or bad weather conditions. We calculate the transit durations for the remaining two complete transit light curves in the R band, and the results are 0.1084 ± 0.0018 days in 2008

and $0.1101^{+0.0028}_{-0.0019}$ days in 2009, which are identical to each other when considering their error bars. So, we cannot learn more from the present TDV study.

5. SUMMARY

We have made new photometric observations for the transit events of the exoplanetary system WASP-11/HAT-P-10, and refined its physical properties using the MCMC technique based on the new photometric observations and published photometric and RV observations. Compared with the previous study for this system, the new results confirm that the planet orbit is circular ($e = 0$), and the planet parameters are refined as $M_p = 0.526 \pm 0.019 M_J$ and $R_p = 0.999^{+0.029}_{-0.018} R_J$, which results in an average density $\rho_p = 0.526^{+0.035}_{-0.046} \rho_J$, which is between the values derived by previous investigators (Bakos et al. 2009; West et al. 2009). The new planet mass value confirms the measurement of West et al. (2009), and the new radius value confirms the result of Bakos et al. (2009), which solve the problem that the parameters of the system disagree with each other in the two discovery papers. Through the analysis of 19 mid-transit epochs carefully collected, the orbital period of WASP-11b/HAT-P-10b is refined to be $P = 3.72247669(181)$ days, and no obvious TTV signal can be found from the present ($O - C$) study of its orbital period. Due to the large gaps in the ($O - C$) data, created by an unseen phase of the target WASP-11/HAT-P-10 for many nights every year, it is necessary to accumulate longer term ($O - C$) information so as to study its overall TTV behavior in the future.

We thank the 1 m telescope operators and a few graduate students of Yunnan Observatories for their support and help during our observations. We are grateful to the anonymous referee for constructive suggestions and comments, which resulted in a large improvement of the manuscript. This work was supported by the National Natural Science Foundation of China (No. 10873031), Chinese Academy of Sciences (project KJCX2-YW-T24), and the special grant from Sik Sik Yuen of Hong Kong, China.

REFERENCES

- Agol, E., Steffen, J., Sari, R., et al. 2005, *MNRAS*, **359**, 567
 Bakos, G. A., Pal, A., Torres, G., et al. 2009, *ApJ*, **696**, 1950
 Charbonneau, D., Brown, T. M., Latham, D. W., et al. 2000, *ApJL*, **529**, L45
 Claret, A. 2000, *A&A*, **363**, 1081
 Claret, A. 2004, *A&A*, **428**, 1001
 Collier Cameron, A., Pollacco, D., Street, R. A., et al. 2006, *MNRAS*, **373**, 799
 Collier Cameron, A., Wilson, D. M., West, R. G., et al. 2007, *MNRAS*, **380**, 1230
 Enoch, B., Collier Cameron, A., Parley, N. R., et al. 2010, *A&A*, **516**, A33
 Ford, E. B. 2005, *AJ*, **129**, 1706
 Holman, M. J., & Murray, N. W. 2005, *Sci*, **307**, 1288
 Irwin, J. B. 1952, *ApJ*, **116**, 211
 Kipping, D. M. 2009a, *MNRAS*, **392**, 181
 Kipping, D. M. 2009b, *MNRAS*, **396**, 1797
 Mandel, K., & Agol, E. 2002, *ApJL*, **580**, L171
 Pollacco, D., Skillen, I., Collier Cameron, A., et al. 2008, *MNRAS*, **385**, 1576
 Sada, P. V., Deming, D., Jennings, D. E., et al. 2012, *PASP*, **124**, 212
 Tamuz, O., Mazeh, T., & Zucker, S. 2005, *MNRAS*, **356**, 1466
 Wang, X.-B., Gu, S.-H., Collier Cameron, A., et al. 2013, *RAA*, **13**, 593
 West, R. G., Collier Cameron, A., Hebb, L., et al. 2009, *A&A*, **502**, 395
 Winn, J. N., Holman, M. J., Carter, J. A., et al. 2009, *AJ*, **137**, 3826